# FLOW OF A TWO-DIMENSIONAL LIQUID METAL JET IN A STRONG MAGNETIC FIELD

MOLOKOV, S.[1] and REED, C.B.[2]
[1]*Coventry University, School of Mathematical and Information Sciences, Priory Street, Coventry CV1 5FB, UK, e-mail: s.molokov@coventry.ac.uk*
[2]*Argonne National Laboratory, 9700 South Cass Avenue, Argonne, IL 60439, USA, e-mail: cbreed@anl.gov*

## 1. Introduction and formulation

A combined effect of surface tension, gravity, inertia and a transverse nonuniform magnetic field on the steady, two-dimensional jet (or curtain) flow is studied with reference to liquid metal divertors of tokamaks [1] and coating flows [2]. Here main fundamental aspects of the flow are presented. More details on the assumptions, analysis and results are given in [3].

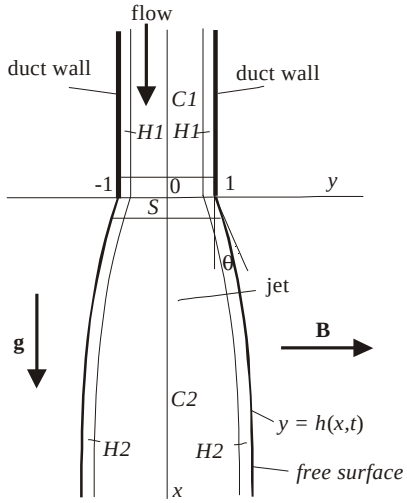


**Fig. 1** *Schematic diagram of a 2-D jet flow*

Consider a steady flow of a viscous, electrically conducting, incompressible fluid in a jet pouring downward in the $x^*$-direction (the direction of gravity) from a nozzle (Fig. 1). Here $(x^*, y^*, z^*)$ are Cartesian co-ordinates. Dimensional quantities are denoted by letters with asterisks, while their dimensionless counterparts - with the same letters, but without the asterisks. For $x^* < 0$ the flow is between two parallel plates located at $y^* = \pm a^*/2$. The location of the free surface is defined as follows: $y^* = \pm h^*(x^*)$, $x^* > 0$. The flow is supposed to be symmetric with respect to $y^*$, and thus the region $y^* > 0$ only is considered. The flow occurs in the presence of a strong, transverse magnetic field $\mathbf{B}^* = B_0^* B(2x^*/a^*)\hat{\mathbf{y}}$, where $B_0^*$ = constant is the induction of the magnetic field in the far upstream region. Laterally the flow is confined by perfectly conducting sidewalls at $z^* = \pm L^*$, which are connected through a resistor, so that the resulting constant electric field $E^*$ is supposed to be given. Sufficiently far from the sidewalls current flows in the $z^*$-direction only, while the flow may be considered 2-D, in the $(x^*, y^*)$-plane [4].

The characteristic values of the length, the fluid velocity ($u$,$v$), the electric current density $j_z$, the electric field and the pressure $p$ are $a^*/2$, $v_0^* = Q^*/a^*$ (average velocity in the duct), $\sigma v_0^* B_0^*$, $v_0^* B_0^*$ and $a^* \sigma v_0^* B_0^{*2}$, respectively. In the above, σ, ρ, ν are the electrical conductivity, density and kinematic viscosity of the fluid, resp., and $Q^*$ is the flow rate. Then the dimensionless, two-dimensional, inductionless equations governing the flow are [5]:

$$Ha^{-2}\nabla^2 u - j_z B(x) = \partial_x p - \delta + N^{-1}\{u\partial_x u + v\partial_y u\}, \qquad (1a)$$

$$Ha^{-2}\nabla^2 v = \partial_y p + N^{-1}\{u\partial_x v + v\partial_y v\}, \quad j_z = E + uB(x), \quad \partial_x u + \partial_y v = 0, \quad (1b\text{-}d)$$

where $Ha = a^* B_0^* (\sigma/\rho\nu)^{1/2}$ is the Hartmann number; $N = a^* \sigma B_0^{*2}/\rho v_0^*$ is the interaction parameter; $\delta = \rho g/\sigma v_0^* B_0^{*2}$ expresses the ratio of gravity to the electromagnetic (EM) force [5]. Typical values of parameters for various flows are given in [3], [5]. Both *Ha* and *N* are usually high, but for some flow regimes $N < 1$; δ may be as low as ~ $10^{-4}$-$10^{-6}$ (negligible gravity), or as high as ~1. Therefore, in the following it is treated as an $O(1)$ parameter.

The boundary conditions at the duct walls are the no-slip conditions. At the free surface the kinematic and dynamic boundary conditions hold. Far upstream the flow is fully developed. Finally, the solution is normalized using the condition of a fixed flow rate.

In the following Eqs. (1) are analysed for high values of *Ha*. First the inertialess flow is studied in Sec. 2 for an arbitrary jet thickness and curvature of the free surface. Then in Sec. 3 slender inertial jet is studied, which requires $|\partial_x h| << 1$.

## 2. Inertialess jet flow for high *Ha*

In this section the problem defined by Eqs. (1) is analysed for $Ha >> 1$, $N \to \infty$. In the following all the flow variables denote their core values. Terms $O(Ha^{-1})$ are neglected. In a sufficiently strong magnetic field the flow region splits into the following main subregions (Fig. 1): the cores *C1*, *C2*, the Hartmann layers *H1*, *H2* of thickness $O(Ha^{-1})$ at the walls and the free surface, respectively, and the internal parallel layer *S* at $x = 0$ of thickness $O(Ha^{-1/2})$.

The analysis of the flow in the cores and the Hartmann layers yields the following results.

In the *duct region* one gets $u = 1$, $v = 0$, i.e. the Hartmann flow holds up to the junction, while pressure "absorbs" all variations of the field with *x*.

For the *jet region* the analysis leads to the following nonlinear third-order equation for function $h(x)$:

$$\lambda\kappa' = EB - \delta + B^2 h^{-1}, \qquad (2)$$

where $\kappa = h''\left[1 + h'^2\right]^{-3/2}$ is the curvature of the free surface; parameter $\lambda = \gamma/(a^{*2} B_0^{*2} \sigma v_0^*)$ expresses the ratio of the surface tension and EM forces; $\gamma$ is the surface tension coefficient, $' = d/dx$. As $\lambda$ varies in a wide range ($\sim 10^{-7}$-$10^{0}$) [3] it is treated as an $O(1)$ parameter. If $\lambda$ is low, the EM force dominates surface tension. Nevertheless, as will be shown below even if $\lambda << 1$, the surface tension cannot always be neglected.

The other core variables are expressed in terms of *h* as follows: $u(x) = h^{-1}(x)$, $v(x, y) = -y\partial_x u$, $p(x) = -\lambda\kappa$. The constant pressure of the surrounding medium is set to zero.

As there is a corner at $x = 0$, $y = 1$, the fluid will tend to be attached to it [2], i.e.

$$h = 1 \quad \text{at } x = 0, \qquad (3)$$

while $h'(0) = \tan\theta$ is arbitrary provided the angle $\theta$ satisfies Gibbs' inequality [2].

The conditions far downstream from the duct exit depend on the asymptotics of *B* at infinity. For $B \to B_\infty = \text{const.}$ as $x \to \infty$, the boundary conditions are:

$$h \to \beta, \quad h' \to 0 \quad \text{as } x \to \infty, \qquad (4a,b)$$

where $\beta = B_\infty^2(\delta - EB_\infty)^{-1}$. In this case parameter $\beta$ has a meaning of being half the constant jet thickness far downstream. More generally, parameter $\beta^{-1}$ may be thought of as an efficient gravity modified by the Lorentz force. In the far downstream region the flow variables are $u_\infty = \delta B_\infty^{-2} - EB_\infty^{-1}$, $v_\infty = 0$, $j_{z\infty} = \delta B_\infty^{-1}$, $p_\infty = 0$, so that the fluid flows with a constant velocity in a jet of a uniform thickness determined by the field in the downstream region.

The flow in the parallel layer, for which there is a balance of viscous and EM forces, is similar to that in a linear duct expansion [6] and thus is not discussed here.

Solutions of Eqs. (2)-(4) for various limiting cases are presented in Table 1.

The jet profile is uniform for $B = 1$, $\beta = 1$ (Case *I*).

Solution of linearized Eq. (2) is given in row *II*. In particular, it shows that surface tension acts over a distance $O(\lambda^{1/3})$ from the nozzle.

Case *III* corresponds to negligible surface tension. In particular, for $\delta = 0$ and $E = -1$ (zero net current far upstream in the duct), one gets $h = B$, i.e. the jet expands if *B* increases or contract if *B* decreases along the flow. This is in excellent agreement with the numerical solution [10].

Even if $\lambda << 1$, surface tension effects are negligibly small in the whole domain only if solution *III* satisfies the boundary condition (2).

**Table 1.** *Jet profiles for various limiting cases. Inertialess flow*

| | *Conditions* | *h* | *Notation* |
|---|---|---|---|
| *I* | $B = 1, \beta = 1$ | 1 | - |
| *II* | $B = 1, \ \lvert\beta - 1\rvert << Ha^{-1/2}, \ \lvert h'\rvert << 1$ | $\beta - e^{-\eta}\Delta h$ | $\eta = x\lambda^{-1/3}$ |
| *III* | $\lambda = 0$ | $B^2(x)/[\delta - EB(x)]$ | - |
| *IV* | $B = 1+mx, \delta = 0, E = -1$ | $1+mx$ | $m$ – field gradient |

If $\lambda \neq 0$ and for a *uniform field* ($B = 1$), Eq. (2) becomes:

$$\lambda\kappa' = h^{-1} - \beta^{-1}. \qquad (5)$$

The boundary-value problem defined by Eqs. (5), (2), (3) has been solved numerically. The results of calculations for $\lambda = 10^{-4}$ and for several values of $\beta$ are shown in Fig. 2. Linearized solutions are also shown in the figure with broken lines.

For values of $|\beta - 1|$ higher than those in Fig. 2 the solution breaks down. To investigate this effect calculations have been performed for $\beta = 1.25$ and several values of $\lambda$ integrating an initial-value problem from down- into the up- stream direction. We let calculations run beyond the level $h = 1$ until the solution either reaches $h = 0$, or terminates (Fig. 3). The starting point is arbitrary ($X = 0$ in Fig. 3) as Eq. (5) is invariant with respect to translation along the $x$-axis. It is seen that for $\lambda < 1$ the solution terminates at certain points, where $|h'| \to \infty$, $|h''| \to -\infty$, while $\kappa$ remains finite. For $\lambda < 0.003$ the solution terminates above $h = 1$. Thus, for sufficiently low values of $\lambda$ the steady flow obeying the pinned-end boundary condition (3) is not possible. The situation for which the solution breaks down first will be called critical, characterised by $\lambda_{cr}$, $\beta_{cr}$.

If curvature is linearized, $\kappa \approx h''$, the solution exists for all values of $\lambda$ and $\beta$ (Fig. 3).

Variation of angle $\theta = \tan^{-1}(h'(0))$ with $\lambda$ for expanding jets is shown in Fig. 4. For any value of $\beta$, as $\lambda$ decreases, $\theta$ eventually becomes $+90^{o}$.

If parameters $\lambda$ and $\beta$ are beyond critical several possibilities arise: (i) the flow becomes unstable; (ii) the slope never becomes equal to $\pi/2$, being adjusted in the parallel layer; (iii) pinned-end boundary condition is violated. Here we study scenario (iii).

For $\beta < 1$ (contracting jet) the point of attachment may move upstream (Fig. 4). At the solid walls a contact angle, $\theta_0$, must be specified. If wettability of walls is poor, then $\theta_0 > \pi/2$. This corresponds to a sub-critical flow (Fig. 5a), which for super-critical values of parameters is not permitted. Thus the point of attachment will move upstream until *the whole duct drains*.

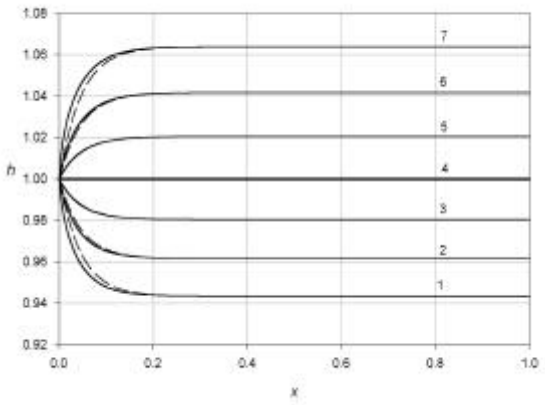


**Fig. 2** *Variation of h with x for* $\lambda = 10^{-4}$, $B = 1$, *and for* $\beta = 1.064$ (1), 1.042 (2), 1.02 (3), 1 (4), 0.981 (5), 0.962 (6), 0.943 (7).

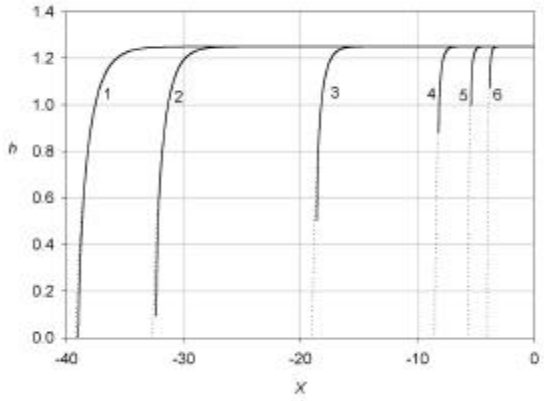


**Fig. 3** *The results of shooting from downstream for* $\beta = 1.25$, $B = 1$, *and for* $\lambda = 1$ (1), 0.5 (2), 0.1 (3), 0.01 (4), 0.003 (5), 0.001 (6)

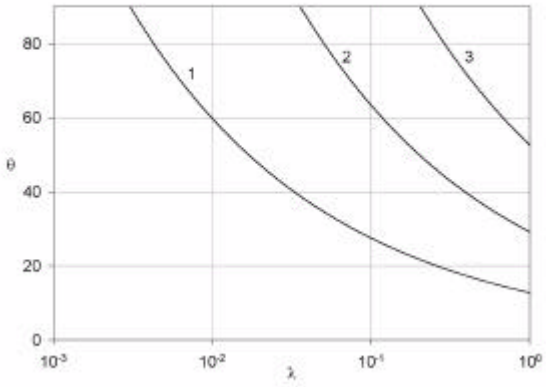


**Fig. 4** *Variation of* θ (deg) with λ for $B = 1$ *and for* $\beta = 1.25$ (1), 1.67 (2), 2.5 (3).

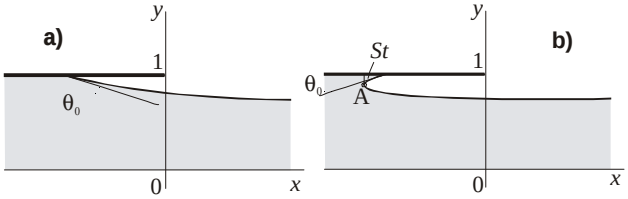


**Fig. 5** *Schematic diagram of the post-critical profiles of a contracting jet for poor (a) and good (b) wettability of walls.*

If wettability is good ($\theta_0 < \pi/2$), a new equilibrium is possible (Fig. 5b). In this case regions of stagnant fluid (*St*) are formed, in which there is an equilibrium between the effective gravity and surface tension: $\lambda\kappa' = -\beta^{-1}$. At points *A* in Fig. 5b $|h'| \to \infty$, *h'* changes its sign, while κ matches that of a critical solution.

What exactly will happen for an expanding jet largely depends on the geometry of the flow at $x = 0$ and again on the wettability of the solid walls. If walls at $x = 0$ are also present, they will be partially flooded (Fig. 6). The parallel layer becomes that in a sudden expansion [7]. Several other possibilities have been discussed in [3]. Other flows studied are straight jet pouring into a draining duct (Fig. 6), a jet from one duct into another, and that in a liquid bridge.

Ultimately, the dynamics of the transition and the supercritical flow itself will depend on such experimental conditions as wall roughness, cleanness, etc. Therefore, experimental studies of the dynamics contact angles in MHD flows may be crucial.

Concerning nonuniform magnetic fields, they can be efficiently used to tailor the jet profile. Indeed, it is possible to obtain profile of the jet with a desired thickness $h(x)$. For $h(0)=1$, solving Eq. (2) for $B(x)$ gives $B(x) = \frac{1}{2}\{-Eh + [E^2h^2 + 4(\delta - \lambda h\kappa')]^{1/2}\}$. A solution for a linearly expanding jet is presented in Table 1, line *IV*. Other results are presented below.

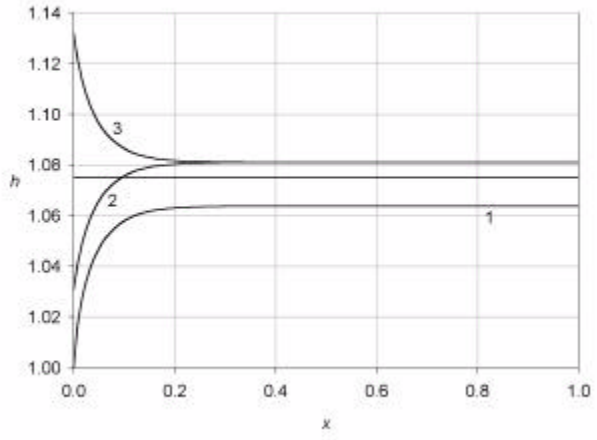


**Fig. 6** *Flows for* $B = 1$, $\lambda = 10^{-4}$*: subcritical flow for* $\beta = 1.064$ (1), *and super-critical flows for* $\beta = 1.07$, and for $\theta_0 = 150^o$ (2), $30^o$ (3). Straight line: $\beta_{cr} = 1.075$.

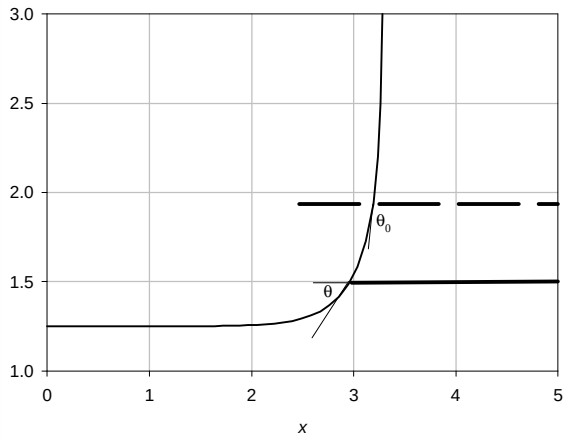


**Fig. 7** *Straight jet pouring into the draining duct for* $B = 1$, $\lambda = 10^{-4}$, $\beta = 1.25$. *Pinned-end conditions (thick straight line); given contact angle (broken straight line).*

**Table 2.** *Jet profiles for B = 1 and for various limiting cases. Slender inertial jet*

| | *Conditions* | *h* | *Notation* |
|---|---|---|---|
| *I* | $\beta = 1$ | 1 | - |
| *II* | $\lvert\beta - 1\rvert << 1,\ \lvert h'\rvert << 1$ | $\beta - e^{-l\eta}\Delta h$ | $\tau = \lambda^{-1/3}N^{-1},\ l = r^{-1/3}(12\tau - r^{2/3})/6,$ $\eta = x\lambda^{-1/3},\ r = -108 + 12\sqrt{12\tau^3 + 81}$ |
| *III* | $\lambda = 0$ | $Nx = -\beta^{-1}\ln\lvert g\rvert + 1 - h^{-1}$ | $g = (h^{-1} - \beta^{-1})/(1 - \beta^{-1})$ |
| *IV* | $\beta \to \infty,\ \lambda = 0$ | $[1 - Nx]^{-1}$ | - |
| *V* | $\beta \to 0,\ \lambda = 0$ | $(2Nx\beta^{-1} + 1)^{-1/2}$ | - |

## 3. Slender inertial jet

Consider now inertial, laminar flow; see the discussion in [3]. The inertial term $N^{-1}u\partial_x u$ in Eq. (1a) is retained, while all other inertial terms in Eqs. (1a,b) are neglected. This requires that the jet is slender ($h' << 1$, i.e. linearized curvature) [3]. Similar analysis to that in Sec. 2 yields a third-order ordinary differential equation for the jet thickness as follows:

$$\lambda h''' = -N^{-1}B^2h^{-3}h' + B^2h^{-1} + \delta - EB. \qquad (50)$$

Solutions of Eqs. (50), (2), (3) for $B = 1$ and for various limiting cases are presented in Table 2. The jet profile is uniform for $\beta = 1$ (Case *I;* curve 5 in Fig. 8), as in Sec. 2.

Solution of linearized Eq. (2) is given in row *II*. It shows that surface tension acts over a distance $O(\lambda^{1/3}l)$. In this region there is a balance between the EM, inertial and surface tension forces. For $N >> \lambda^{-1/3}$ one gets $\tau \to 0,\ l \to 1$, i.e. the flow becomes inertialess. For $N << \lambda^{-1/3}$ one gets $\tau \to \infty,\ l \sim \tau^{-1}$, from which follows that $l\eta \sim Nx$.

For l = 0 the solution has been presented in an implicit form (Case *III*, Fig. 8). For all cases presented in Fig. 8, except for $\beta = 0$, inertia acts over a distance of about $2N^{-1}$, which is less than one value of the characteristic length.

For $\beta \to \infty$ gravity is fully balanced by *E*, while the jet is completely diverted in the $\pm y$-direction at a distance $x = N^{-1}$ (Case *IV*). This is similar to a submerged 2-D jet studied in [8].

If $\beta \to 0$ (high gravity) the jet becomes thinner along the flow, while the fluid accelerates (Case *V*). If $E = 0$, this becomes the classical solution for an ordinary hydrodynamic jet pulled by gravity [9]; parameter $N/\beta$ being the inverse of the Froude number.

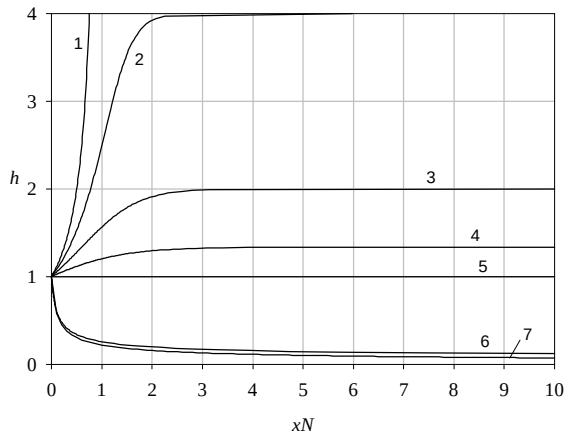


**Fig. 8** Slender inertial jet for $B = 1$, $\lambda = 0$ and for $\beta = \infty$ (1), 4 (2), 2 (3), 0.57 (4), 1 (5), 10 (6), and pure-gravity solution (Case *V*) for $\beta = 10$.

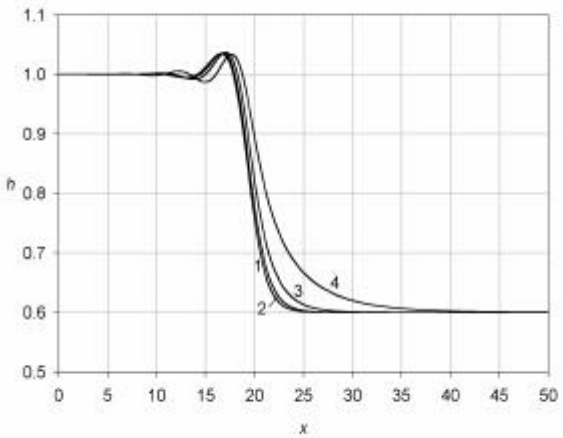


**Fig. 9** Slender inertial jet in a step-like field for $\lambda = 1$, $x_0 = 20$, $E = -1$, $B_\infty = 0.6$, $\zeta = 1$, $\delta = 0$ and for $N = \infty$ (1), 10 (2), 3 (3), 1 (4).

Now let us discuss the effect of *nonuniform* fields. In the following we will consider a family of step-like fields: $B = \frac{1}{2}(B_\infty + 1) + \frac{1}{2}(B_\infty - 1)\tanh\zeta(x - x_0)$. Parameter $\zeta$ defines the gradient of the field; $x_0$ defines the position where $B$ is an average value of $B_\infty$ and 1. The results for $\lambda = 1$, $x_0 = 20$, $E = -1$, $B_\infty = 0.6$, $\zeta = 1$are shown in Fig. 9. As point $x_0$ is located far into the jet region, the jet profile at the nozzle is a constant. As in Sec. 2 the jet thickness largely follows the field profile. However, surface-tension induced "wiggles" are present. Their intensity increases with increasing $\lambda$ and $N$ [3]. If the flow remains steady, inertia is important for $N < 3$ only. This conclusion is valid for all cases studied in [3], i.e. velocities up to 10m/s and field down to 1T, except for an increasing, high-gradient field. This may result in a flip-over of the jet profile at some distance from the nozzle. For gradually varying fields this effect does not occur.

## 4. Conclusions

If the flow is *inertialess* and the field downstream is uniform, the jet thickness tends to a certain constant $\beta$. In this region the Lorentz force compensates gravity, while variations of pressure and thus surface tension force vanish. Therefore in contrast to ordinary hydrodynamic flows it is possible to create a curtain of a constant thickness.

Concerning the effect of *surface tension*, it acts over a distance $O(\lambda^{1/3})$ from the nozzle. For $\lambda << 1$ surface tension acts in a layer at the nozzle, where the flow is governed by the EM-surface tension balance. The surface tension tends to smooth the jump in the constant jet profile downstream and that at the nozzle. As one moves from downstream region towards the nozzle, $|\kappa|$ monotonically increases. If the jump to be smoothed is too high, the solution ceases to exist. This situation is called critical. For $\lambda << 1$ sub-critical solutions exist only for a very narrow range of the jump $|\beta\text{-}1|$. If the value of $\lambda$ or $|\beta\text{-}1|$ are beyond critical, partial flooding of the nozzle walls, or draining of the duct are expected. The critical solutions give the upper limit for the pinned-end condition to hold. If the advancing or receding contact angles for a wall are not $0^o$ or $180^o$, the Gibbs' condition will be violated for the values of $|\beta\text{-}1|$ and $\lambda$ less than critical, so the range of existence of a sub-critical flow is even narrower.

If the magnetic field is *non-uniform*, the jet tends to expand if the field increases, and contract if the field decreases; the jet thickness being proportional to $B(x)$. Partial flooding of walls is also expected. For high-gradient field surface-tension induced wiggles have been observed in the jet profile, which increase in magnitude with increasing $\lambda$.

It has been shown that for the steady flow *inertial effects* are generally not important for $N > 3$. The analysis presented here is valid for a single-component field and for a two-dimensional jet. The work on jets of finite cross-section and flow stability is in progress.

**Acknowledgement:** This work has been supported by the Office of Fusion Energy Sciences, U.S. Department of Energy, under Contract No. W-31-109-ENG-38.

## References

[1] **R. Mattas et al.** (2000) *Fus. Eng. Des*. **49-50**, 127-134.
[2] **Liquid film coating** (1997) *Eds.: S.F.Kistler, P.M.Schweitzer, (Chapman& Hall: London), 1997.*
[3] **S. Molokov and C.B. Reed** (2002) *ANL Report No. ANL/TD/TM02-29.*
[4] **P.R. Hays and J.S. Walker** (1984) *Trans. ASME. E: J. Appl. Mech.* **106**, 13-18.
[5] **S. Molokov and C.B. Reed** (1999) *ANL Report No. ANL/TD/TM99-08.*
[6] **Hunt, J.C.R. and Leibovich, S.** (1967) *J. Fluid Mech* **28**, 241-260.
[7] **Molokov, S.** (2000) *Proc. PAMIR Conf., Presquile de Giens, France, September 18-22, 2000, p. 573-578.*
[8] **H.K. Moffatt and J. Toomre** (1967) *J. Fluid Mech.* **30**, 65-82.
[9] **D.R. Brown** (1961) *J. Fluid Mech.* **10**, 297-305.
[10] **S. Aleksandrova, S. Molokov, C.B. Reed** (2002) *ANL Report No. ANL/TD/TM02-30.*